Repeatability of Quantitative ^{18}F-DCFPyL PET/CT Measurements in Metastatic Prostate Cancer

Bernard H.E. Jansen[1,2], Matthijs C.F. Cysouw[1,3], André N. Vis[2], Reindert J.A. van Moorselaar[2], Jens Voortman[3], Yves J.L. Bodar[1,2], Patrick R. Schober[4], N. Harry Hendrikse[1,5], Otto S. Hoekstra[1], Ronald Boellaard[1], and D.E. Oprea-Lager[1]

[1]Department of Radiology and Nuclear Medicine, Cancer Center Amsterdam, Amsterdam University Medical Centers, VU University, Amsterdam, The Netherlands; [2]Department of Urology, Cancer Center Amsterdam, Amsterdam University Medical Centers, VU University, Amsterdam, The Netherlands; [3]Department of Medical Oncology, Cancer Center Amsterdam, Amsterdam University Medical Centers, VU University, Amsterdam, The Netherlands; [4]Department of Anesthesiology, Amsterdam University Medical Centers, VU University, Amsterdam, The Netherlands; and [5]Department of Clinical Pharmacology and Pharmacy, Cancer Center Amsterdam, Amsterdam University Medical Center, VU University, Amsterdam, The Netherlands

Quantitative evaluation of radiolabeled prostate-specific membrane antigen (PSMA) PET scans may be used to monitor treatment response in patients with prostate cancer (PCa). To interpret longitudinal differences in PSMA uptake, the intrinsic variability of tracer uptake in PCa lesions needs to be defined. The aim of this study was to investigate the repeatability of quantitative PET/CT measurements using ^{18}F-DCFPyL ([2-(3-(1-carboxy-5-[(6-^{18}F-fluoro-pyridine-3-carbonyl)-amino]-pentyl)-ureido)-pentanedioic acid], a second-generation ^{18}F-PSMA-ligand) in patients with PCa. **Methods:** Twelve patients with metastatic PCa were prospectively included, of whom 2 were excluded from final analyses. Patients received 2 whole-body ^{18}F-DCFPyL PET/CT scans (median dose, 317 MBq; uptake time, 120 min) within a median of 4 d (range, 1–11 d). After semiautomatic (isocontour-based) tumor delineation, the following lesion-based metrics were derived: mean, peak, and maximum tumor-to-blood ratio; SUV_{mean}, SUV_{peak}, and SUV_{max} normalized to body weight; tumor volume; and total lesion uptake (TLU). Additionally, patient-based total tumor volume (TTV) (sum of PSMA-positive tumor volumes) and total tumor burden (TTB) (sum of all lesion TLUs) were derived. Repeatability was analyzed using repeatability coefficients (RC) and intraclass correlation coefficients. Additionally, the effect of point-spread function (PSF) image reconstruction on the repeatability of uptake metrics was evaluated. **Results:** In total, 36 ^{18}F-DCFPyL PET–positive lesions were analyzed (≤5 lesions per patient). The RCs for mean, peak, and maximum tumor-to-blood ratio were 31.8%, 31.7%, and 37.3%, respectively. For SUV_{mean}, SUV_{peak}, and SUV_{max}, the RCs were 24.4%, 25.3%, and 31.0%, respectively. All intraclass correlation coefficients were at least 0.97. Tumor volume delineations were quite repeatable, with an RC of 28.1% for individual lesion volumes and 17.0% for TTV. TTB had an RC of 23.2% and 33.4% when based on SUV_{mean} and mean tumor-to-blood ratio, respectively. Small lesions (<4.2 cm³) had worse repeatability for volume measurements. The repeatability of SUV_{peak}, TLU, and all patient-level metrics was not affected by PSF reconstruction. **Conclusion:** ^{18}F-DCFPyL uptake measurements are quite repeatable and can be used for clinical validation in future treatment response assessment studies. Patient-based TTV may be

preferred for multicenter studies because its repeatability was both high and robust to different image reconstructions.

Prostate cancer (PCa) is the second most common cancer in men worldwide, with an estimated annual number of deaths exceeding 350,000 (*1*). Prostate-specific membrane antigen (PSMA) PET is increasingly used for PCa diagnostics (*2*). PSMA is a class II transmembrane glycoprotein that provides a valuable target for radiolabeled imaging, as its expression is upregulated in malignant prostate cells and associated with aggressive disease characteristics (*3*). Because of greater availability, the ^{68}Ga-labeled PSMA tracers have been studied most frequently to date, demonstrating high detection rates for metastatic disease (*2,4*). Alternatively, ^{18}F-labeled tracers have been developed, including ^{18}F-DCFPyL (2-(3-(1-carboxy-5-[(6-^{18}F-fluoro-pyridine-3-carbonyl)-amino]-pentyl)-ureido)-pentanedioic acid), a second-generation small-molecule ligand that strongly binds to PSMA (*5,6*). The ^{18}F-radionuclide provides for PET images with a higher resolution than is possible with ^{68}Ga, because of a shorter positron range and higher positron yield (*2*).

Quantitative analysis of PSMA uptake may be used to predict or evaluate treatment response, as changes in PSMA uptake over time may indicate a response to treatment or progression of disease (*7–9*). Recently, we performed a full pharmacokinetic analysis of ^{18}F-DCFPyL to validate simplified methods to quantify tumor uptake. Tumor-to-blood ratios (TBRs; the activity in the tumor normalized to the whole-blood activity on PET) were found to best describe tumor uptake (*10*). For reliable use of quantitative PSMA PET metrics in clinical practice, it is important to determine their repeatability. Only changes that exceed random variability should be interpreted as a treatment response or disease progression. To the best of our knowledge, this was the first study on the day-to-day variability in ^{18}F-DCFPyL uptake in PCa lesions. Our aim was to evaluate the repeatability of quantitative ^{18}F-DCFPyL PET/CT measurements in patients with metastatic PCa.

MATERIALS AND METHODS

Patients

Twelve patients were prospectively included in the Amsterdam UMC between January and May 2019. The inclusion criteria were histologically proven PCa, at least 2 metastases as detected by any imaging modality, and 1 or more metastases at least 1.5 cm in size (to minimize partial-volume effects). Patients with multiple malignancies and claustrophobia were excluded.

The study was approved by the ethical review board of the Amsterdam UMC, and all subjects gave written informed consent. The trial was registered as EudraCT number 2017-000344-18 and The Netherlands Trial Registry number 6477. Personal and demographic data on age, height, body weight, Gleason score, and prostate-specific antigen level (ng/mL) at the time of PET/CT, as well as information on prior therapy, were collected.

Data Acquisition

All patients underwent 2 ^{18}F-DCFPyL PET/CT scans within a median of 4 d (range, 1–11 d). PET/CT imaging adhered to routine clinically used protocols. ^{18}F-DCFPyL was synthesized under good-manufacturing-practice conditions at the Amsterdam UMC Radionuclide Center, using the precursor of ABX GmbH ([11]). No fasting was required, and no diuretics were administered before imaging. PET was performed using a European Association of Nuclear Medicine Research Ltd. (EARL)–calibrated hybrid Ingenuity TF scanner (Philips Healthcare) ([12,13]). Our imaging protocol included a target injected ^{18}F-DCFPyL dose of 300 MBq, with an uptake interval of 120 min after injection. First, a CT scan was obtained for attenuation correction (30–120 mAs; 120 kV). Next, whole-body PET acquisitions were acquired from mid thigh to skull base (4 min per bed position).

The images were corrected for decay, scatter, random coincidences, and photon attenuation and were reconstructed using (EARL1-compliant ([13])) ordered-subsets expectation maximization with time of flight (3 iterations; 33 subsets). Additionally, images were post-processed using a point-spread-function (PSF) reconstruction (Lucy–Richardson iterative deconvolution) ([14]). Using a NEMA-NU-2 image-quality phantom, the full width at half maximum of this reconstruction was calibrated at 7.0 mm for adequate signal recovery complying with the EARL2 guidelines ([15]).

Data Analysis

All scans were controlled for image quality ([16]) and were visually interpreted by an experienced nuclear medicine physician, who identified suspected PCa metastases in bone or lymph nodes. The lesions were semiautomatically delineated using in-house–developed software (ACCURATE-tool, previously benchmarked against commercially available image-analysis tools ([17])) using a 50% isocontour of SUV_{peak} (sphere of 1.2-cm diameter, positioned to maximize its mean value) with correction for local background uptake to obtain volumes of interest (VOIs) ([18]). Blood activity concentrations (for TBR calculation) were measured in the ascending aorta using a single-image-slice 3×3 voxel VOI and a 3×3 voxel VOI in 5 consecutive slices ([10]). VOIs were created on both original (EARL1) and PSF (EARL2) reconstructions.

From each VOI, the following metrics were recorded at a lesion level: total tumor volume (TTV, the sum of the delineated tumor volumes within a patient [cm^3]), TBR (tumor VOI activity concentration to blood activity concentration), SUV, and total lesion uptake (TLU). TBR was calculated using the mean, peak, and maximum activity within the VOI. SUV variants included SUV_{max} within the VOI, SUV_{peak} (SUV_{mean} within a 12-mm-diameter sphere positioned within the VOI to yield the highest value), and SUV_{mean} within the VOI. SUV was normalized to body weight. TLU was defined as the lesion SUV_{mean} or mean TBR multiplied by the lesion volume,

yielding SUV TLU and TBR TLU, respectively. Additionally, 2 patient-level metrics were derived: total PSMA-positive TTV and PSMA total tumor burden (TTB, the sum of the SUV TLU and TBR TLU within a patient, yielding SUV TTB and TBR TTB, respectively). As recommended by the PERCIST guidelines for PET response assessment ([19]), and to balance the number of analyzed lesions between patients, for lesion-based analyses we selected the 5 hottest lesions if there were more than 5 PSMA-avid lesions. For patient-level analysis, all suspected PSMA-avid lesions were included.

Statistical Analysis

To assess differences in uptake intervals and injected does between test and retest scans, we used the Wilcoxon signed-rank test for paired data. The repeatability of quantitative PET metrics was quantified using repeatability coefficients (RCs, as percentages). The RCs were calculated as 1.96 times the SD of relative test–retest differences, d, which were calculated as follows:

$$d = \frac{X2 - X1}{\overline{X}} \times 100, \qquad \text{Eq. 1}$$

where $X1$ and $X2$ are the lesion- or patient-level metrics on day 1 (test) and day 2 (retest), respectively. $\overline{X}$ is the average between $X1$ and $X2$. Bland–Altman plots were used for visual inspection of test–retest differences. Also, intraclass correlation coefficients (2-way mixed model with an absolute agreement definition) were calculated between test and retest data. The Pitman–Morgan test was used to test for differences in repeatability between paired data (correlated variances) ([20]), with α set at 0.05. P values were corrected for multiple comparisons using the Holms–Bonferroni method ([21]). The Levene test was used to compare variances of independent groups in subgroup analysis (bone vs. lymph node metastases, $>4.2 \ cm^3$ lesions vs. $<4.2 \ cm^3$ lesions). SPSS, version 22.0 (IBM), and Excel (Microsoft) worksheets were used for statistical analyses.

RESULTS

Patients

Twelve patients were enrolled, of whom 2 could not be analyzed. The characteristics and disease stage of the 10 patients who were finally evaluated are presented in Table 1. Seven (70%) patients were receiving androgen-deprivation therapy (luteinizing hormone–releasing hormone agonist), all of whom had been treated for at least 3 mo at the time of PET. In 1 excluded patient, a reliable comparison of the ^{18}F-DCFPyL scans was impeded by significant radiolysis of the tracer (evident from a visually altered biodistribution and highly abnormal bone uptake ([16])). The radiolysis was likely caused by a relatively high radioactivity concentration in the production batch (268 MBq/mL), combined with a long interval between delivery of the tracer and injection (>3 h). Tracer logistics and storage were improved after this incidental finding, and no other radiolysis problems occurred during this study. Another patient was excluded because of unconfirmed malignancy found on post hoc CT-guided histologic biopsy during clinical follow-up for 2 highly suggestive bone lesions on ^{18}F-DCFPyL PET. There were no significant differences between uptake intervals, injected doses, and injected masses between test and retest scans ($P = 0.799$, 0.499, and 0.878, respectively).

Repeatability of Lesion-Level Metrics

In total, 36 ^{18}F-DCFPyL PET–avid lesions were analyzed, including 21 bone lesions (58.3%), 12 lymph node metastases (33.3%), and 3 intraprostatic foci (8.3%). Descriptive values for the analyzed PET parameters are shown in Table 2 (PSF reconstruction data

<div style="display:flex">

TABLE 1
Patient and Scan Characteristics of Patients Included in Repeatability Analysis ($n = 10$)

Characteristic	Data
Age (y)	74 (61–79)
Initial Gleason score	8 (6–9)
PSA at PET/CT (ng/mL)	9 (1–2,796)
Length (cm)	178 (168–192)
Weight (kg)	88 (68–94)
PCa stage	
Primary metastatic	2 (20.0%)
Biochemically recurrent	3 (30.0%)
Castration-resistant	5 (50.0%)
Analyzed lesion type	
Bone	21 (58.3%)
Lymph node	12 (33.3%)
Intraprostatic	3* (8.3%)
Androgen deprivation at PET/CT	7 (70.0%)
Prior docetaxel	3 (30.0%)
Injected activity (MBq)	
Test	317 (280–331)
Retest	313 (254–341)
Uptake time (min)	
Test	120 (118–153)
Retest	122 (111–149)
Test–retest difference[†]	
Injected activity (MBq)	28 (8–63)
Uptake time (min)	3 (0–22)

*Differences were not significant ($P > 0.05$).
[†]2 intraprostatic foci in 1 patient.
Qualitative data are numbers followed by percentages in parentheses; continuous data are median followed by range in parentheses.

TABLE 2
Descriptive Data of Lesion and Patient-Based Uptake Metrics on Test and Retest Scans

	Test		Retest	
Parameter	Median	IQR	Median	IQR
Lesion level				
Volume	4.6	2.8–8.7	4.6	2.5–8.6
SUV_{mean}	16.6	9.5–24.4	17.1	9.7–28.0
SUV_{peak}	21.7	10.5–28.3	21.6	11.4–32.2
SUV_{max}	28.1	16.0–41.0	29.8	17.2–51.2
Mean TBR	13.4	7.1–24.1	14.6	8.6–22.7
Peak TBR	17.7	7.7–28.4	18.8	9.8–26.7
Maximum TBR	25.0	11.7–40.9	23.6	14.1–38.8
SUV TLU	85.6	32.3–192.7	80.1	30.1–194.0
TBR TLU	67.6	24.6–189.4	66.7	23.5–152.6
Patient level				
TTV	21.4	10.6–63.2	21.8	10.3–69.7
SUV TTB	317.8	70.4–1,920.7	285.5	70.6–1,846.4
TBR TTB	236.6	63.2–1,920.1	224.9	68.2–1,720.0

IQR = interquartile range.

</div>

between the repeatability of metrics derived from bone and those derived from lymph node metastases were observed ($P = 0.06–0.98$). Only volume measurements had a significantly different repeatability for lesions larger than 4.2 cm^3 versus those smaller than 4.2 cm^3 (RC, 17.6% and 36.8%, respectively; $P = 0.015$).

TABLE 3
Repeatability of Lesion- and Patient-Based ^{18}F-DCFPyL Uptake Metrics

Parameter	Mean test–retest difference (%)	RC (%)	ICC	95% CI
Lesion level				
Volume	−1.1	28.1	1.00	0.99–1.00
SUV_{mean}	1.0	24.4	0.99	0.98–0.99
SUV_{peak}	1.8	25.3	0.99	0.97–0.99
SUV_{max}	1.9	31.0	0.97	0.94–0.99
Mean TBR	1.9	31.8	0.98	0.96–0.99
Peak TBR	2.6	31.7	0.98	0.96–0.99
Maximum TBR	2.7	37.3	0.97	0.94–0.98
SUV TLU	−0.1	32.1	0.99	0.98–1.00
TBR TLU	−3.5	39.3	0.98	0.96–0.99
Patient level				
TTV	−2.2	17.0	1.00	0.99–1.00
SUV TTB	−0.2	23.2	0.99	0.97–1.00
TBR TTB	−2.1	33.4	0.98	0.91–0.99

ICC = intraclass correlation coefficient; CI = confidence interval.

are in Supplemental Table 1; supplemental materials are available at http://jnm.snmjournals.org). The best repeatability was observed for SUV_{mean} (RC, 24.4%) and SUV_{peak} (RC, 25.3%). SUV_{max} had poorer repeatability (RC, 31.0%; Table 3), but the differences between the repeatability of SUVs were not significant ($P = 0.06–0.60$). Blood activity derived from a 1-slice and 5-slice VOI had a repeatability of 23.1% and 17.3%, respectively. Consequently, calculating TBR using 5-slice blood measurements had better repeatability than single-slice measurements (RC, 31.7%–37.3% vs. 34.1%–40.1%) and was used henceforth. Overall, TBRs had worse repeatability than SUVs, but only for mean TBR was repeatability significantly lower than that of SUV_{mean} (RC, 31.8%, vs. 24.4%, $P = 0.03$; Fig. 1).

The repeatability of semiautomatic tumor volume measurement was 28.1%. The repeatability of TBR TLU (RC, 39.3%) was nonsignificantly lower than that of SUV TLU (RC, 32.1%; $P = 0.08$). Bland–Altman plots did not demonstrate a skewed variability, but the variability of SUV and TBR tended to be less for higher values (Fig. 2). In the subgroup analysis, no significant differences
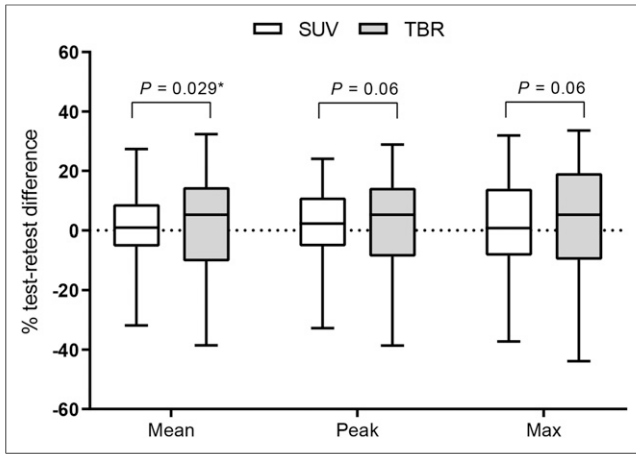
FIGURE 1. Test–retest variability of SUV and TBR variants. Significant differences have been indicated with asterisk (Holms-Bonferroni–corrected P values). Differences in repeatability between SUVs and between TBRs were not significant.

Repeatability of Patient-Level Metrics

The highest repeatability was observed for TTV (RC, 17%). SUV TTB had better repeatability than TBR TTB, albeit nonsignificantly (RC, 23.2% vs. 33.4%; $P = 0.19$). Bland–Altman plots demonstrated no skewed variability (Fig. 3).

Effect of PSF Reconstruction on Repeatability

PSF reconstruction worsened repeatability significantly for the TBRs, SUV_{mean}, and SUV_{max} ($P \leq 0.005$; Supplemental Table 2). However, the repeatability of tumor volume (RC, 32.0%; $P = 0.43$), SUV_{peak} (RC, 27.8%; $P = 0.15$), SUV TLU (RC, 30.3%; $P = 0.62$), and TBR TLU (RC, 41.3%; $P = 0.70$) was not affected. Notably, for none of the patient-level metrics was repeatability significantly affected by the PSF reconstruction ($P = 0.15$–0.59; Supplemental Table 2).

DISCUSSION

In this study, we investigated the repeatability of ^{18}F-DCFPyL uptake and volume measurements in metastatic PCa patients. Knowledge of the day-to-day variation in these metrics is indispensable for the use of ^{18}F-DCFPyL metrics as novel biomarkers to assess response to systemic treatments. We conclude that ^{18}F-DCFPyL uptake metrics are highly repeatable (intraclass correlation coefficient ≥ 0.97) and are thus suited for response monitoring. SUV metrics tend to have higher repeatability than TBRs. The best repeatability was observed for patient-based TTV measurements.

In routine static PET acquisitions, ^{18}F-DCFPyL pharmacokinetics are quantified most accurately using the TBR (*10*), which demonstrated a repeatability of 31.8% in this study. Hence, a change in TBR exceeding 32% may indicate a change in tumoral ^{18}F-DCFPyL uptake that exceeds the physiologic variability, for
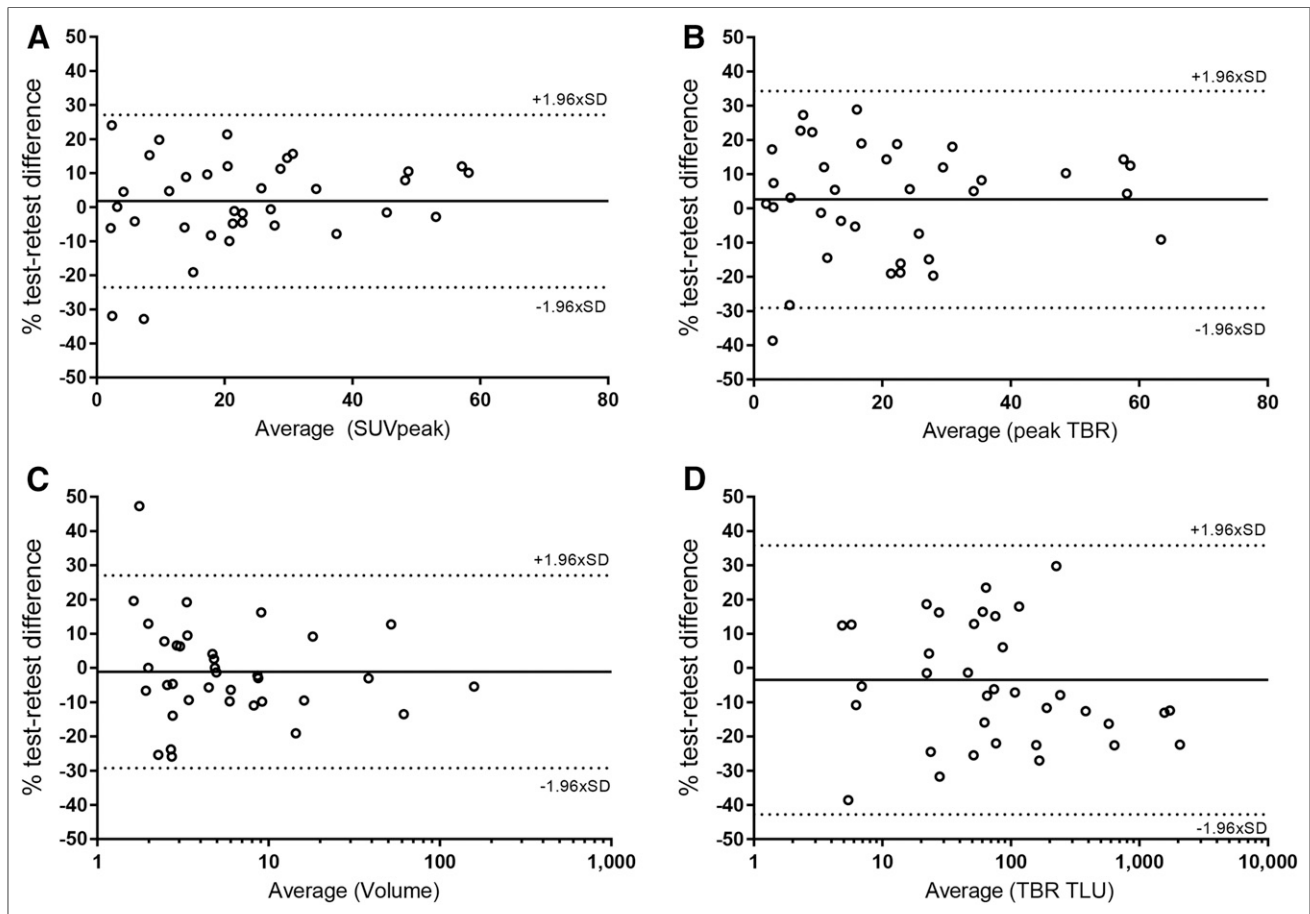

FIGURE 2. Bland–Altman plots of lesion-level metrics: SUV_{peak} (A), peak TBR (B), volume (C), and TBR TLU (D). y-axis in C and D were log-scaled for visual interpretation.
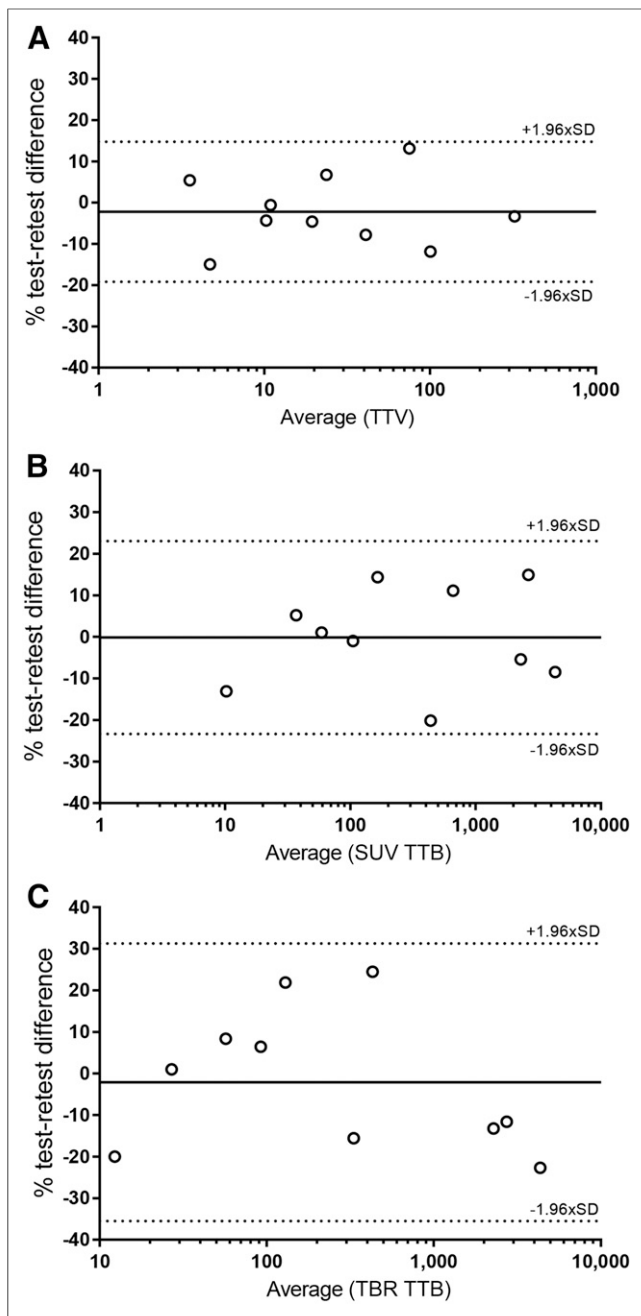
FIGURE 3. Bland–Altman plots of patient-level metrics TTV, SUV TTB, and TBR TTB. *y*-axes were log-scaled for visual interpretation.

in ^{18}F-DCFPyL during response monitoring. These findings are in line with those for other PCa radiotracers (^{18}F-fluoromethylcholine, ^{18}F-fluordihydrotestosterone), for which tumor uptake measurements normalized to blood-pool activity are more accurate metrics for tracer quantification than SUV but have worse repeatability (*23,24*). When all these considerations are taken together, TBR may be preferred over SUV metrics despite its lower repeatability, which we recently illustrated in a clinical case (*22*). The higher variability of TBR than of SUV will have a negative impact on response assessment only in patients with small tumor volumes with small treatment effect sizes.

Interestingly, the semiautomatically delineated TTV demonstrated the highest overall repeatability (RC, 17%). These favorable outcomes are likely explained by the high tumor-to-background ratio that ^{18}F-DCFPyL provides (and PSMA tracers in general), permitting reliable automatic or semiautomatic identification of tumor extent. On a lesion basis, however, variability in volume measurements was larger (RC, 28.1%), which can at least partly be explained by the volume dependency of its variability. The high repeatability of TTV may be of benefit for longitudinal assessments of total PSMA burden in patients receiving systemic treatments. Especially for PSMA-targeted radioligand therapies (e.g., ^{177}Lu-PSMA), assessment of changes in the TTV as a whole, instead of individual lesion responses, may be clinically useful.

In multicenter studies, use of different PET/CT systems with varying image-reconstruction protocols requires quantitative metrics that are robust to such factors. Advanced reconstruction methods may improve lesion detection (*25*), but repeatability may be hampered by the inherent image noise propagation. In line with previous observations for ^{18}F-fluorodihydrotestosterone (*26*), we observed lower repeatability for several metrics when using an image reconstruction method with improved signal recovery, adhering to newer imaging guidelines (EARL2). However, the repeatability of SUV_{peak}, TLU, and patient-level measurements was not affected by the PSF reconstruction, rendering them fit for use in multicenter studies for which PET imaging protocols differ between centers. Because blood activity measurements are susceptible to noise, the repeatability of TBR was negatively affected by PSF reconstruction. Overall, non-PSF reconstruction images (EARL1-compliant) may therefore be preferred for quantitative assessment.

Our study had limitations, most notably the small patient sample. Still, the results were in line with findings on other ^{18}F-labeled PCa radiotracers, as well as ^{18}F-FDG (*19,23,24*). Factors contributing to the total variability in quantitative PET metrics include biologic variation in tracer uptake, image noise, deviations in protocol between scans, and the analysis software used. We acknowledge the patients' heterogeneity in disease stages (primary metastatic disease, biochemical recurrence, castration resistance), but subgroup analysis per disease stage was not feasible at the current sample size. We have no reason to assume that tracer uptake variability attributable to tumor biology will differ between disease stages, however. In our single-center evaluation, only a single type of PET scanner and analysis software package was used; multicenter variability may be higher. We welcome repetition of our study by other investigators using ^{18}F-DCFPyL in their own center, or even in a multicenter setting, to validate our current findings in a larger cohort. In the present study, the tracer uptake time and injected doses for both the test and the retest scans were similar (Table 1). Because our pharmacokinetic data indicated that tumor ^{18}F-DCFPyL uptake continues to rise at 120 min after injection (*10*), test–retest

such reasons as disease progression, treatment response, a true flare phenomenon, or an imaging-protocol deviation. The repeatability of tumor SUV_{mean} was superior to that of TBR (Fig. 1). This is logically explained for TBR including an additional measurement (with a certain variability), that is, blood-pool activity (RC, 17.3%). Still, in our pharmacokinetic analysis, we concluded that SUV measurements do not universally correlate with the underlying ^{18}F-DCFPyL pharmacokinetics (K_i), as intrapatient tumor volumes appear to affect the bioavailability of the tracer (a so-called sink effect) (*10,22*). At higher tumor loads, SUV tends to underestimate ^{18}F-DCFPyL uptake in lesions, whereas TBR (partly) corrects for this difference and thus better reflects changes

variability might be higher in clinical practice, where uptake times between scans may vary more. Clinical imaging protocols for ^{18}F-DCFPyL regarding uptake time intervals, total scan duration, and patient positioning (i.e., feet first or head first) should be stringently adhered to, especially in response assessment studies.

CONCLUSION

In this study, we assessed the repeatability of quantitative ^{18}F-DCFPyL PET/CT measurements in patients with metastatic PCa, concluding that ^{18}F-DCFPyL uptake metrics are quite repeatable. The variability limits proposed in this study should be validated in future clinical studies. To this end, any change in TBR exceeding 32% can be considered a change in tracer uptake beyond physiologic day-to-day variability (in the case of comparable image-acquisition parameters). Additionally, because TTV measurements are highly repeatable (RC, 17%), they may be specifically suited to longitudinal assessment of PSMA-targeted radioligand therapy effects. The repeatability of SUV_{peak}, TLU, and patient-level metrics (TTV and TTB) of ^{18}F-DCFPyL uptake is robust to differences in image reconstructions.

DISCLOSURE

KEY POINTS

QUESTION: What is the repeatability of quantitative ^{18}F-DCFPyL PET/CT measurements in patients with metastatic PCa?

PERTINENT FINDINGS: In this prospective test–retest study, we demonstrated that quantitative ^{18}F-DCFPyL PET/CT measurements are quite repeatable and may thus be used for treatment response monitoring.

IMPLICATIONS FOR PATIENT CARE: If there are comparable image-acquisition parameters, any change in TBR exceeding 32% will indicate a change beyond physiologic day-to-day variability that should trigger further evaluation. TTV measurements may be specifically suited to longitudinal assessment of PSMA-targeted radioligand therapies.

REFERENCES

1. Bray F, Ferlay J, Soerjomataram I, Siegel RL, Torre LA, Jemal A. Global cancer statistics 2018: GLOBOCAN estimates of incidence and mortality worldwide for 36 cancers in 185 countries. *CA Cancer J Clin.* 2018;68:394–424.
2. Rowe SP, Gorin MA, Allaf ME, et al. PET imaging of prostate-specific membrane antigen in prostate cancer: current state of the art and future challenges. *Prostate Cancer Prostatic Dis.* 2016;19:223–230.
3. Perner S, Hofer MD, Kim R, et al. Prostate-specific membrane antigen expression as a predictor of prostate cancer progression. *Hum Pathol.* 2007;38:696–701.
4. Perera M, Papa N, Christidis D, et al. Sensitivity, specificity, and predictors of positive ^{68}Ga-prostate-specific membrane antigen positron emission tomography in advanced prostate cancer: a systematic review and meta-analysis. *Eur Urol.* 2016;70:926–937.
5. Robu S, Schmidt A, Eiber M, et al. Synthesis and preclinical evaluation of novel ^{18}F-labeled Glu-urea-Glu-based PSMA inhibitors for prostate cancer imaging: a comparison with ^{18}F-DCFPyl and ^{18}F-PSMA-1007. *EJNMMI Res.* 2018;8:30.
6. Chen Y, Pullambhatla M, Foss CA, et al. 2-(3-{1-carboxy-5-[(6-[18]fluoro-pyridine-3-carbonyl)-amino]-pentyl}-ureido)-pentanedioic acid, [18]DCFPyL, a PSMA-based PET imaging agent for prostate cancer. *Clin Cancer Res.* 2011;17:7645–7653.
7. Fendler WP, Eiber M, Beheshti M, et al. ^{68}Ga-PSMA PET/CT: joint EANM and SNMMI procedure guideline for prostate cancer imaging—version 1.0. *Eur J Nucl Med Mol Imaging.* 2017;44:1014–1024.
8. Gupta M, Choudhury PS, Rawal S, Goel HC, Rao SA. Evaluation of RECIST, PERCIST, EORTC, and MDA criteria for assessing treatment response with Ga68-PSMA PET-CT in metastatic prostate cancer patient with biochemical progression: a comparative study. *Nucl Med Mol Imaging.* 2018;52:420–429.
9. Seitz AK, Rauscher I, Haller B, et al. Preliminary results on response assessment using ^{68}Ga-HBED-CC-PSMA PET/CT in patients with metastatic prostate cancer undergoing docetaxel chemotherapy. *Eur J Nucl Med Mol Imaging.* 2018;45:602–612.
10. Jansen BHE, Yaqub M, Voortman J, et al. Simplified methods for quantification of ^{18}F-DCFPyL uptake in patients with prostate cancer. *J Nucl Med.* 2019;60:1730–1735.
11. Ravert HT, Holt DP, Chen Y, et al. An improved synthesis of the radiolabeled prostate-specific membrane antigen inhibitor, [^{18}F]DCFPyL. *J Labelled Comp Radiopharm.* 2016;59:439–450.
12. Kolthammer JA, Su KH, Grover A, Narayanan M, Jordan DW, Muzic RF. Performance evaluation of the Ingenuity TF PET/CT scanner with a focus on high count-rate conditions. *Phys Med Biol.* 2014;59:3843–3859.
13. Boellaard R, Delgado-Bolton R, Oyen WJ, et al. FDG PET/CT: EANM procedure guidelines for tumour imaging—version 2.0. *Eur J Nucl Med Mol Imaging.* 2015;42:328–354.
14. Tohka J, Reilhac A. Deconvolution-based partial volume correction in raclopride-PET and Monte Carlo comparison to MR-based method. *Neuroimage.* 2008;39:1570–1584.
15. Kaalep A, Sera T, Rijnsdorp S, et al. Feasibility of state of the art PET/CT systems performance harmonisation. *Eur J Nucl Med Mol Imaging.* 2018;45:1344–1361.
16. Jansen BHE, Kramer GM, Cysouw MCF, et al. Healthy tissue uptake of ^{68}Ga-prostate specific membrane antigen (PSMA), ^{18}F-DCFPyL, ^{18}F-fluoromethylcholine (FCH) and ^{18}F-dihydrotestosterone (FDHT). *J Nucl Med.* 2019;60:1111–1117.
17. Boellaard R. Quantitative oncology molecular analysis suite: ACCURATE [abstract]. *J Nucl Med.* 2018;59(suppl 1):1753.
18. Frings V, Yaqub M, Hoyng LL, et al. Assessment of simplified methods to measure ^{18}F-FLT uptake changes in EGFR-mutated non-small cell lung cancer patients undergoing EGFR tyrosine kinase inhibitor treatment. *J Nucl Med.* 2014;55:1417–1423.
19. Wahl RL, Jacene H, Kasamon Y, Lodge MA. From RECIST to PERCIST: evolving considerations for PET response criteria in solid tumors. *J Nucl Med.* 2009;50(suppl 1):122S–150S.
20. Pitman E. A note on normal correlation. *Biometrika.* 1939;31:9–12.
21. Holm S. A simple sequentially rejective multiple test procedure. *Scand J Stat.* 1979;6:65–70.
22. Cysouw MCF, Jansen BHE, Yaqub M, et al. Letter to the editor re: semiquantitative parameters in PSMA-targeted PET imaging with [^{18}F]DCFPyL—impact of tumor burden on normal organ uptake. *Mol Imaging Biol.* 2020;22:15–17.
23. Oprea-Lager DE, Kramer G, van de Ven PM, et al. Repeatability of quantitative ^{18}F-fluoromethylcholine PET/CT studies in prostate cancer. *J Nucl Med.* 2016;57:721–727.
24. Vargas HA, Kramer GM, Scott AM, et al. Reproducibility and repeatability of semi-quantitative ^{18}F-fluorodihydrotestosterone (FDHT) uptake metrics in castration-resistant prostate cancer metastases: a prospective multi-center study. *J Nucl Med.* 2018;59:1516–1523.
25. Jansen BHE, Jansen RW, Wondergem M, et al. Lesion detection and interobserver agreement with advanced image reconstructions for ^{18}F-DCFPyL PET/CT in patients with biochemically recurrent prostate cancer. *J Nucl Med.* 2020;61:210–216.
26. Cysouw MCF, Kramer GM, Heijtel D, et al. Sensitivity of ^{18}F-fluorodihydrotestosterone PET-CT to count statistics and reconstruction protocol in metastatic castration-resistant prostate cancer. *EJNMMI Res.* 2019;9:70.